A Journal of the Gesellschaft Deutscher Chemiker

Angewandte International Edition

GDCh

Chemie

www.angewandte.org

Accepted Article

Title: Chiral Phosphoric Acids in Metal-Organic Frameworks with Enhanced Acidity and Tunable Catalytic Selectivity

Authors: Xu Chen, Hong Jiang, Yong Cui, Jianwen Jiang, Yan Liu, Wei Gong, Xing Han, Xu Li, Bang Hou, Fanfan Zheng, and Xiaowei Wu

To be cited as: *Angew. Chem. Int. Ed.* 10.1002/anie.201908959
Angew. Chem. 10.1002/ange.201908959

Link to VoR: http://dx.doi.org/10.1002/anie.201908959
http://dx.doi.org/10.1002/ange.201908959

WILEY-VCH

WILEY-VCH

RESEARCH ARTICLE

Chiral Phosphoric Acids in Metal-Organic Frameworks with Enhanced Acidity and Tunable Catalytic Selectivity**

Xu Chen,[a]+ Hong Jiang,[a]+ Xu Li,[b] Bang Hou,[a] Wei Gong,[a] Xiaowei Wu,[a] Xing Han,[a] Fanfan Zheng,[a] Yan Liu,[a]* Jianwen Jiang,[b]* and Yong Cui[a]*

Abstract: New heterogeneous Brønsted acid catalysts with high activity and selectivity are critically needed to substitute precious acid-based catalysts for the sustainable production of fine and commodity chemicals. However, the advance in synthetic methodology for the preparation of such highly desirable catalysts remains a huge scientific challenge. Herein, we report the incorporation of chiral phosphoric acids into indium-based metal-organic frameworks (In-MOFs) by sterically preventing them from coordination. This concept leads to the synthesis of three chiral porous 3D In-MOFs with different network topologies constructed from three enantiopure 1,1'-biphenol-phosphoric acid derived tetracarboxylate linkers. More importantly, all the uncoordinated phosphoric acid groups are periodically aligned within the channels and display significantly enhanced acidity compared to the non-immobilized acids. This facilitates the Brønsted acid catalysis of asymmetric condensation/amine addition and imine reduction. The enantioselectivities can be tuned (up to > 99% ee) by varying the substituents to achieve a nearly linear correlation with the concentrations of steric bulky groups in the MOFs. Density-functional theory calculations suggest that the framework provides a chiral confined microenvironment that dictates both selectivity and reactivity of chiral MOFs.

Introduction

As one versatile class of eco-friendly heterogeneous catalysts, porous solid Brønsted acids have been extensively explored for many challenging and practically important reactions in chemical and petrochemical processes.[1] However, presumably due to the lacking of structural uniformity and designed catalytic sites, the traditional solid acid systems normally show poor selectivity,[2] especially in asymmetric organic reactions. Consequently, most high value-added enantiopure chemicals are still catalyzed by homogeneous catalysts.[3] The requirement for the development of new chiral solid acid catalysts may be realized by MOFs for their structural diversity, uniformity and permanent porosity.[4] MOFs have been extensively explored as catalysts for asymmetric catalysis.[5,6] Among them MOFs adopting the concept of using privileged chiral ligands/catalysts provide an efficient and straightforward strategy for enantioselective processes.[5d,5g,6,7a-7c] The applications, however, have been mainly focused on Lewis acidic catalysts and rarely for Brønsted acid catalysis.[5e-5h,6] To date, only a few catalytically active chiral MOF-based Brønsted acid catalysts have been reported albeit with low to moderate enantioselectivity (5-84% ee).[7b-7f] In general, it is very difficult to retain a strong Brønsted acid site such as phosphoric acid in MOFs, mainly due to spontaneous deprotonation of the acids in solution, which leads to direct metal-acid coordination. [8] Deprotonation of the acids could be avoided by using a strong acid solution for MOF synthesis.[9] Unfortunately, with a few notable exceptions such as MIL-100 and MIL-101,[10] most of the reported MOFs are decomposed under such harsh conditions. It remains a challenge to design chiral Brønsted acid type of MOF catalysts. To address this issue, here we show that phosphoric acids can be introduced into MOFs by sterically protecting them from coordination.

Chiral phosphoric acids derived from axially biaryls such as 1,1'-binaphthol (BINOL) and 1,1'-biphenol have been recognized as one of the most versatile organocatalysts capable of affording numerous enantioselective transformations.[10] Generally, steric bulky substituents at 3,3'-positions of the BINOL or biphenol skeleton exhibit distinct advantages for enantioselectivity, which have a dual role of providing bulky as well as tuning the electronics of the catalysts.[12] We have synthesized several dicarboxylate ligands based on 1,1'-biphenol-2,2'-phosphoric acid with steric bulky groups at the 3,3'-position, having their metal ions coordinated with both carboxylate and phosphonate groups forming MOFs that contain the conjugate base form of phosphoric acid.[13] We surmise that the introduction of steric bulky bridging carboxylate groups at the 3,3'-position of 1,1'-biphenol may protect the phosphoric acids from coordinating with metal ions, whereas the primary functional groups are linked by metal-connecting units to produce extended networks. Herein, we demonstrate as a proof-of-concept of the design of three porous 3D In-MOFs from three newly designed 3,3',5,5'-tetracarboxylate ligands of chiral 1,1'-biphenol-2,2'-phosphoric acid. Despite of their different topological structures, all phosphoric acids are not coordinated with metal ions in the MOFs and are periodically aligned within the channels that endow the frameworks catalytic activity and enantioselectivity in condensation/amine addition and imine reduction. The stereoselectivity is modulated by varying 3,3'-substituents of

[a] X, Chen+, H, Jiang+, B, Hou, W, Gong, X. Wu, X. Han, F. Zheng, Prof. Y. Liu, Prof. Y. Cui
School of Chemistry and Chemical Engineering and State Key Laboratory of Metal Matrix Composites,
Shanghai Jiao Tong University
Shanghai 200240 (China)
E-mail: yongcui@sjtu.edu.cn, liuy@sjtu.edu.cn
[b] X, Li, Prof. J. Jiang
Department of Chemical and Biomolecular Engineering,
National University of Singapore
Singapore 117576, Singapore
E-mail: chejj@nus.edu.sg
[+] These authors contributed equally to this work
[**] This work was financially supported by the National Science Foundation of China (Grants, 21522104, 21620102001, 21875136, and 91856204), the National Key Basic Research Program of China (2016YFA0203400), Key Project of Basic Research of Shanghai (17JC1403100 and 18JC1413200) and Shanghai Rising-Star Program (19QA1404300).

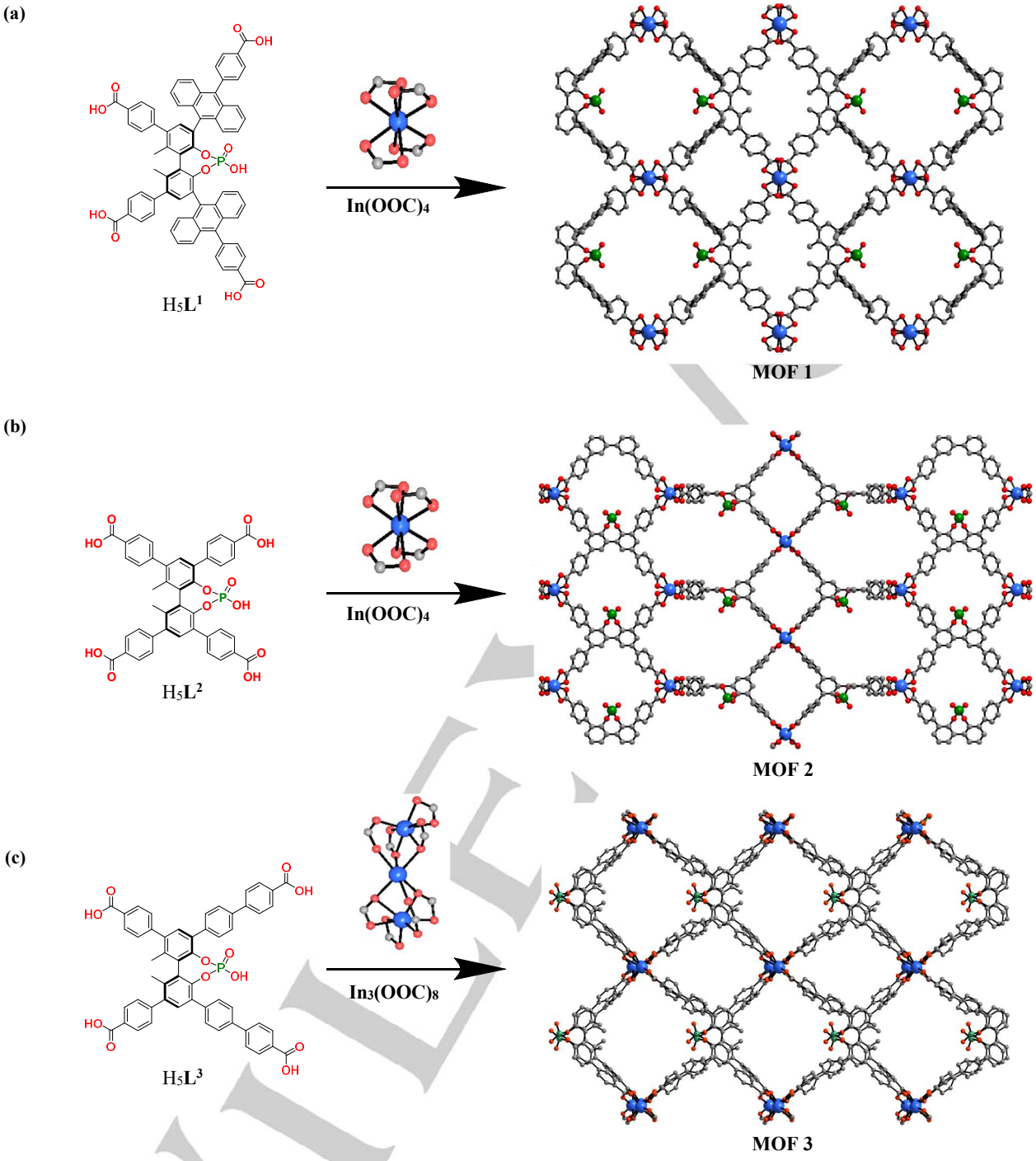

Figure 1. Schematic view of the preparation for MOFs (a) **1**, (b) **2** and (c) **3** (In, blue; O, red; P, green; C, gray. H atoms are omitted for clarity).

biphenol and that the ee values show a nearly linear correlation with the concentrations of bulky groups in the MOFs. A model rationalizing the observed difference is also presented.

Results and Discussion

Synthesis and Characterization. The ligands $H_5\mathbf{L}^1$, $H_5\mathbf{L}^2$ and $H_5\mathbf{L}^3$ were prepared from (*R*)- or (*S*)-6,6'-dimethyl-3,3'-di-*tert*-butyl-5,5'-di(4-methoxycarbonyl)phenyl-1,1'-biphenyl-2,2'-diol in six steps in 24%, 36% and 47% overall yields, respectively. Heating $In(NO_3)_3{\cdot}6H_2O$ and $H_5\mathbf{L}^1$, $H_5\mathbf{L}^2$ or $H_5\mathbf{L}^3$ in a mixed solvent containing dimethylformamide (DMF) at 100 °C produced single crystals of $[Me_2NH_2][In(\mathbf{L}^1)]{\cdot}H_2O{\cdot}2DMF$ (**1**), $[Me_2NH_2]_2[In_2(\mathbf{L}^2)_2]{\cdot}2H_2O{\cdot}DMF$ (**2**), or

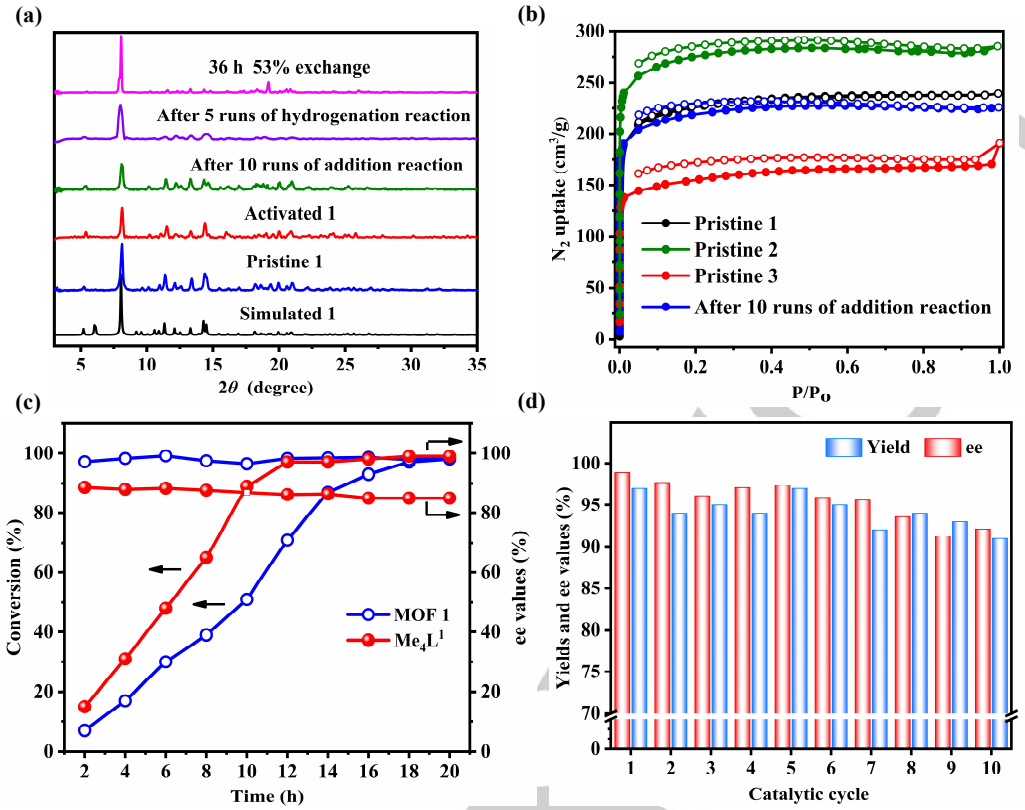

Figure 2. (a) PXRD patterns; (b) N_2 adsorption (filled symbols) and desorption (open symbols) isotherms at 77 K; (c) Conversions and ee values of kinetic experiment with 2-thenaldehyde as substrate and (d) Recycling test of MOF **1** with 2-thenaldehyde as substrate.

$[In_3(\mathbf{L^3})_2][NO_3]\cdot 6.7H_2O\cdot 4DMF$ (**3**), respectively. The obtained In-MOFs were stable in air and insoluble in water and common organic solvents. They were characterized using elemental analysis, IR spectra, and thermogravimetric analysis (TGA). The phase purity of the bulky samples was established by comparing the observed and simulated powder X-ray diffraction (PXRD) patterns.

Single-crystal X-ray diffraction showed that **1** crystallizes in the orthorhombic chiral space group *P*222. The asymmetric unit contains $\mathbf{L^1}$ of 1/2 occupancy and two In ions of 1/4 occupancy. Each In ion is octahedrally coordinated by four carboxylate groups from four different $\mathbf{L^1}$ ligands to form a 4-connected $[In(COO)_4]$ building unit, and each $\mathbf{L^1}$ connects to four $[In(COO)_4]$ nodes (Figures 1a and S4a). Thus, the 3D structure of **1** is built by $[In(COO)_4]$ SBU and tetracarboxylate-phosphoric acid $\mathbf{L^1}$ ligand, which displays a 4-connected topology network with the Schlafli symbol of $[8^6]$ (Figure S3a),. The framework consists of three types of open helical channels along the *a*-axis (1.20 × 1.24 nm^2, 1.05 × 1.26 nm^2 and 0.98 × 1.09 nm^2, measured from van der Waals surfaces), with the largest channel being periodically decorated with free phosphoric acids (Figures 1a and S5a).

Although **2** shares the same $[In(COO)_4]$ building unit and similar 4-connected $\mathbf{L^2}$ ligand as **1**, **2** crystallizes in the hexagonal chiral space group $P6_422$. The asymmetric unit contains one $\mathbf{L^2}$ and one In ion, both of which are in 1/4 occupancy. Each In is coordinated by four bidentate carboxylate groups for four $\mathbf{L^2}$ ligands to form 4-connected $[In(COO)_4]$ SBU (Figure S4b), and each $\mathbf{L^2}$ connects to four In ions. Along the *c*-axis, adjacent In ions are linked by four $\mathbf{L^2}$ to generate a 3_1 helix, leading to an irregular tubule. Each of the helical chain is connected to six adjacent chains by sharing In ions to give a 3D network with 1D hexagonal channel (Figure 1b and S4b). The channels have an opening size of about 1.10 × 1.10 nm^2 and are periodically decorated with uncoordinated phosphoric acids pointing outward (Figures 1b and S5b). With respect to the topology, **2** exhibits a 4-c net with a **qtz** network (Figure S3b), with the presence of two different types of 4-connected nodes, simplified by the ligand and metal node.

3 crystallizes in the monoclinic chiral space group C_2, with the asymmetric unit containing two independent In ions, one In ion of 1/2 occupancy and one independent $\mathbf{L^3}$ ligand. The basic building block is a trinuclear $[In_3]$ unit, which is linked by eight bidentate carboxylate groups of eight $\mathbf{L^3}$ ligands (Figures 1c and S4c). The central In is octahedrally coordinated by six oxygen atoms from six bidentate carboxylate groups, and each terminal In is coordinated by seven oxygen atoms from bidentate carboxylate groups. Each ligand binds to four In_3 units via four bidentate carboxylate groups leaving the free phosphoric acid pointing to the channel. If we do not consider the central metal in the $[In_3]$ units, the structure of **3** presents a 2-fold interpenetrated network with an uninodal topology denoted as **dia**, with the presence of 4-connected nodes, as simplified by the $\mathbf{L^3}$ ligand and In_3 cluster (Figure S3c). On the other hand, a

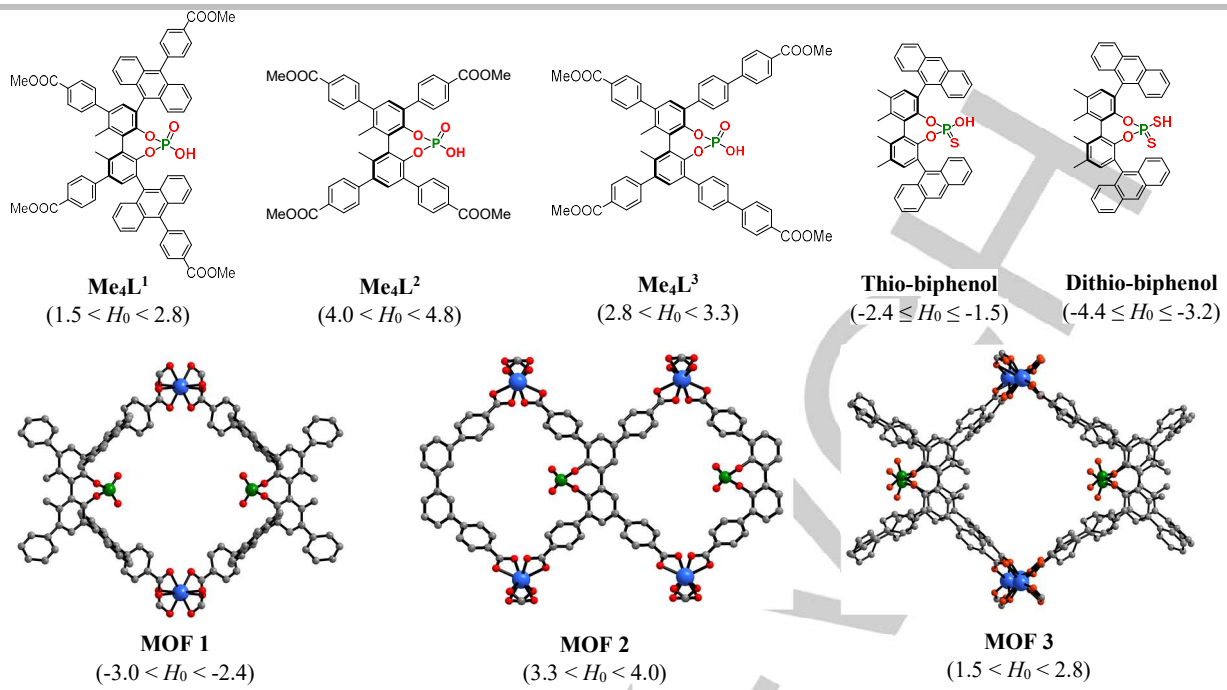

Figure 3. The Hammett acidity of MOFs **1**-**3** and related molecular acids.

different topological simplification could be obtained, if the central In ion is taken into consideration. This simplification results in a 3D 4,8-connected network with the Schlafli symbol of $[4^46^{24}]$ $[4^6]_2$ (Figure S3d), which contains two types of irregular 1D channels with opening sizes of about 1.40 × 1.12 and 1.32 × 0.78 nm^2 (measured from van der Waals surfaces) along the *a*-axis (Figure 1c).The enantiomeric nature of them formed from *R*- and *S*-enantiomers of H_5**L** was confirmed by solid-state circular dichroism (CD) spectra, which exhibit nearly mirror images of each other (Figure S8). Thermogravimetric analysis (TGA) showed the frameworks of **1-3** are thermally stable up to around 400 °C (Figure S9). PXRD showed all three frameworks remain highly crystalline and intact after removal of the guest solvent molecules (Figures 2a, S10a and S10b). Calculations using PLATON indicated that MOFs **1-3** have about 51%, 79% and 68% void volume available for guest inclusion.[14] The permanent porosity was examined by N_2 adsorption measurements at 77 K. The Brunauer-Emmett-Teller (BET) surface areas were estimated to be 699, 847 and 473 m^2/g for **1-3**, respectively (Figures 2b and S11). Dye uptake measurements showed that the open channels of them were well retained in solution (Figures S1, S10a-b and Table S1).

Considering the importance of the catalyst acidity for catalytic applications, the Brønsted acidity of the three In-MOFs and several related organic phosphoric acids was determined by means of the Hammett indicator method.[15] As shown in Figure 3, the molecular catalysts Me_4**L**^{1}, Me_4**L**^{2} and Me_4**L**^{3} were found to have moderate acidity ($1.5 < H_0 < 2.8$, $4.0 < H_0 < 4.8$ and $2.8 < H_0 < 3.3$, respectively), with the order of acidity being consistent with installation of different electron-withdrawing carboxylate groups on biphenol. After assembly into MOFs, the acidity was greatly enhanced ($-3.0 < H_0 < -2.4$, $3.3 < H_0 < 4.0$ and $1.5 < H_0 < 2.8$ for MOFs **1-3**, respectively), as shown in Figure 3. Specifically, MOF **1** showed a color change even in a benzene solution of 4-nitrodiphenylamine, indicating $H_0 \leq -2.40$, which is higher than that of the biphenol thiophosphoric acid ($-2.4 \leq H_0 \leq -1.5$), and even close to that of the strong biphenol dithiophosphoric acid ($-4.4 \leq H_0 \leq -3.2$) (Table S14). The above results suggest that the metal-directed assembly of phosphoric acid catalysts into MOFs is capable of effectively enhancing their Brønsted acidity, giving rise to porous heterogeneous catalysts for fine chemical synthesis. Further study is in progress to understand the origin of the acidity enhancement of the immobilized phosphoric acids.

Heterogeneous Asymmetric Catalysis. Chiral BINOL-derived Brønsted acids have been proved to be highly active for catalyzing a broad range of reactions involving C−C and C−N bonds formation in an enantioselective fashion.[11] The presence of uniformly distributed phosphoric acids within the 1D channel of those present MOFs prompted us to evaluate their catalytic activities in asymmetric addition and reduction of imines.

We first studied the catalytic activity of the MOFs in promoting the asymmetric condensation/amine addition reactions, which provide direct access to optical active 2,3-dihydroquinazolinones with important pharmacological activities.[16] All three MOFs were found to be capable of catalyzing the cascade reaction, whereas **1** gave much higher reactivity and stereoselectivity than **2** and **3**. Specially, after screening a variety of reaction conditions such as catalyst loading, reaction time, temperature and solvents, it was found that, with 5 mol% loading, **1** could catalyze the reaction of benzaldehyde and 2-aminobenzamide to the desired 2,3-dihydroquinazolinone in 96% yield and 99% ee in $CHCl_3$ at 80 °C after 20 h (Table 1, 4a). Under the optimized conditions, a variety of aromatic aldehydes (with substituents at different positions and heteroaromatic aldehydes) were evacuated. In all cases, the catalytic reactions provided the targeted products in 91-97% yields and 94-99.5% ee (Table 1, 4a-4i).

Table 1. Asymmetric condensation/amine addition reaction[a]

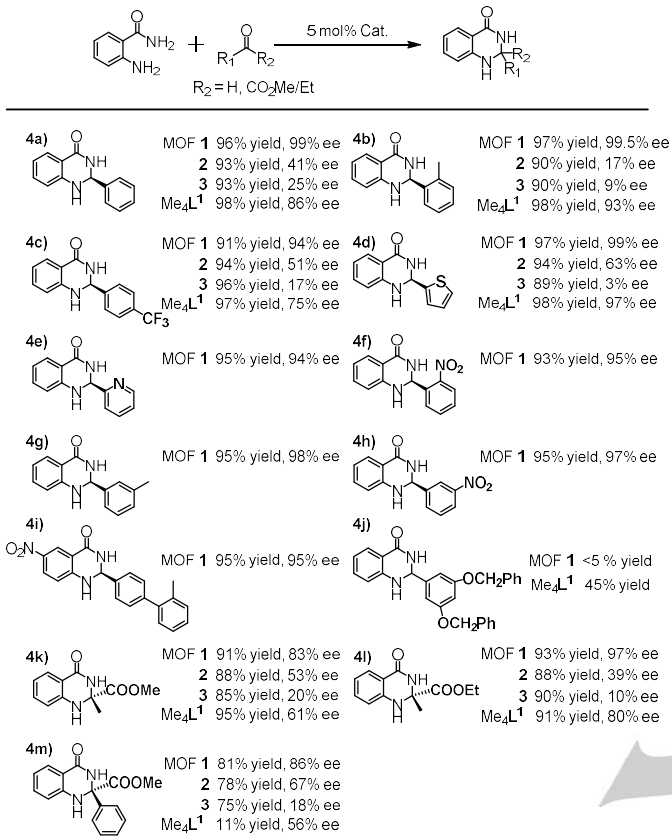

[a] Reaction conditions: Cat. (5 mol %), 2-aminobenzamide (0.15 mmol) and aldehyde/ketone (0.30 mmol), $CHCl_3$ (1 mL), 80 °C / 60 °C. The absolute configurations of the products 4a, 4b, and 4f were assigned as *S* by comparing their HPLC profiles with those reported in literature.[17] 4c, 4d, 4e, 4g, 4h and 4i were assigned were assigned by analogy. The *R* configuration of 4l was defined by single crystal x-ray diffraction. 4k and 4m were assigned by analogy. [b] Isolated yield. [c] Determined by HPLC analysis.

Under identical conditions, MOFs **2** and **3** with different aryl substituents at the 3,3'-positions can also catalyze these reactions, affording 90-94% and 89-96% yields with 17-63% and 3-25% ee, respectively. The ee values are much lower than those obtained with MOF **1**, as presented in Table 1. Interestingly, despite sharing the same less bulky substituents phenyl groups at 3,3'-positions, the ee values obtained with **2** were 8-60% higher than those with **3**, probably due to the different shortest distances between phosphoric acid sites and the framework walls (0.49 nm and 0.92 nm) that lead to different levels of asymmetric induction. The above results indicat that both the local environmental and the position of the phosphoric acids are critically important for enantioselectivities of the MOF catalysts.

To assess the contribution of the MOF structure to the asymmetric catalysis, we examined the catalytic activities of the homogeneous analogue $Me_4\mathbf{L^1}$. Control experiments showed $Me_4\mathbf{L^1}$ (5 mol% loading) gave high yields of the products from the condensation/amine addition reactions, but with much lower ee values than **1** (Table 1, 4a-4d). To further understand the reaction detail, kinetic experiments were performed using 2-aminobenzamide and 2-thenaldehyde as the substrates (Figure 2c). It was found that the reaction catalyzed by $Me_4\mathbf{L^1}$ was faster than that by **1**, but with much low enantioselectivity in the whole process. Although both **1** and $Me_4\mathbf{L^1}$ share the same bulky substituents, the resulting ee values are clearly different for the same reactions under identical conditions. The observed difference in ee values indicates that chiral phosphoric acids of 1,1'-biphenol that together with the In ions, phenyl rings and bulky anthracenyl substituents create a chiral microenvironment in the porous structure, which is believed to be responsible for the observed high enantioselectivity, by concentrating substrates and generating additional steric and electronic effects around the acid active sites.[13]

To further understand the influence of the steric bulky groups on the MOF-base catalysis, we prepared a series of multivariate (MTV) MOFs containing different molar ratios of $\mathbf{L^1}$ and $\mathbf{L^3}$ through a solvent-assistant ligand-exchange approach. The MOFs $\mathbf{1}$-$\mathbf{L^1}_{1-x}$-$\mathbf{L^3}_x$ (X stands for the exchanged ratio) that are unable to access *de novo* were prepared by heating **1** in a MeOH solution of $H_5\mathbf{L^3}$ at 100 °C for a period of time. The ratio of $\mathbf{L^1}$ to $\mathbf{L^3}$ decreases with increasing reaction time, which were determined by ^{1}H NMR after digesting the samples with dilute hydrochloric acid. As shown in Figure 4b, $\mathbf{L^3}$ reaches its equilibrium after 36 h at 53% (Figure S1). Further prolongation of reaction time and exchange of reaction solution with fresh one do not further increase the content of $\mathbf{L^3}$, indicating that a dynamic equilibrium was reached. PXRD showed the resulting MTV-MOFs are all isostructural to the parent MOF crystals (Figures 2a and S10c). Subsequently, we examined their catalytic activities for the reaction between benzaldehyde and 2-aminobenzamide. As shown in Figure 4, as the ratio of $\mathbf{L^3}$ increases, the yields of the product remain constant but the ee values decrease smoothly from 99% for MOF **1** to 58% for $\mathbf{1}$-$\mathbf{L^1}_{0.47}$-$\mathbf{L^3}_{0.53}$. The ee values show a nearly linear correlation with the concentration of steric bulky groups in the MOF catalyst. This result demonstrates that the bulky anthracenyl groups of the biphenol ligand are indeed responsible for the observed high stereoselectivity for the heterogeneous catalyst system.

Multiple experiments were performed to prove the heterogeneity and recyclability of the MOF **1** catalyst. Upon completion of the reaction of 2-aminobenzamide and 2-thenaldehyde, **1** could be recovered by simple filtration and reused at least ten times without any loss of its activity and enantioselectivity (Figures 2a and 2b). After ten cycles, both the PXRD pattern and BET surface area (660 m^2g^{-1}) of **1** remained almost unchanged as compared to the pristine sample (Figures 2b). Secondly, a hot filtration test showed no indication of catalysis by leached homogeneous species. Inductively coupled plasma optical emission spectrometry (ICP-OES) analysis of the product solution indicated almost no loss of In ions (~0.002%) from the structure per cycle.

It should be noted that numerous Brønsted acid catalysts have been explored for the enantioselective synthesis of 2,3-dihydroquinazolinone,[17] but, in most cases, only moderate to

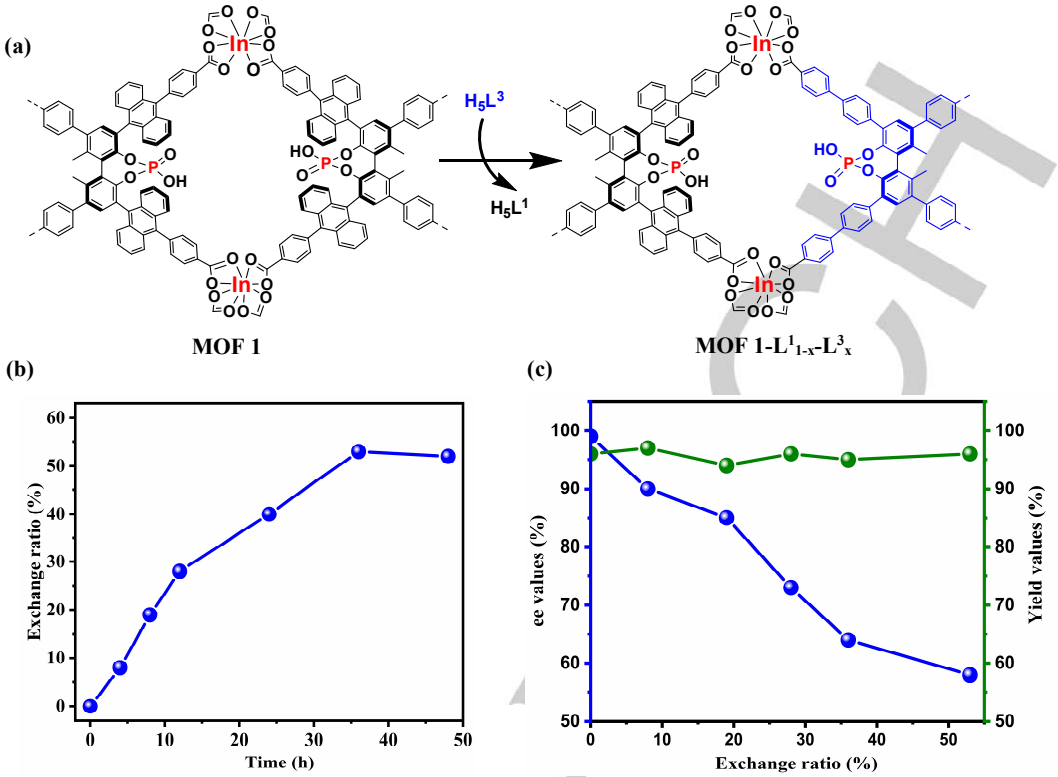

Figure 4. (a) Illustration of the post-synthetic ligand exchange; (b) Exchange ratio depended on the reaction time; (c) Yields and ee values at different exchange ratio in addition reaction with 2-aminobenzamide and benzaldehyde as substrates.

excellent enantioselectivities were observed.[17b-17g] High stereo- and regioselectivity are noteworthy features of the present protocol based on MOF **1**, which is even among the highest values reported for homogeneous phosphoric acid catalysts (Table S8). The synthetic utility of this MOF **1**-based methodology was shown by the synthesis of enantiopure 2-biphenyl substituted 2,3-dihydroquinazolinone (DHQZ) analogue 4i (Table 1, 4i), which was the potent tubulin inhibitor against a number of human cancer cell lines.[16] It was found that **1** loading at 5 mol% catalyzed the asymmetric condensation/amine addition reaction between 2-amino-5-nitrobenzamide and 2'-methylbiphenyl-4-carboxaldehyde in 95% yield and 95% ee. Although the obtained ee was slightly lower than those obtained with homogeneous catalysts,[16a] this new synthetic method only requires a short enatioselective pathway with improved synthesis yield (from 7% to 63%) (Scheme S5).

Despite great efforts, the asymmetric condensation/amine addition of 2-aminobenzamides and ketones has not been well studied, mainly due to the intrinsically low reactivity of ketones.[18] Encouraged by the outstanding catalytic performance of the MOFs, we decided to evaluate their catalytic activities in the condensation/amine addition reactions involving ketones. Although both MOFs and Me_4**L**^{1} were proved to be efficient, only MOF **1** turned out to be promising in term of yields and enantioselectivities for the tested substrates. Specially, with 5 mol% catalytic loading, **1** provided > 90% yields and 83% and 97% ee for two aliphatic ketones (Table 1, 4k and 4l). However, for the substrate with phenyl group, reduced yield and ee value were obtained (Table 1, 4m). Despite that MOFs **2** and **3** could give comparable yields to MOF **1**, their enantioselectivities were significantly reduced (39-67% and 10-20% ee) (Table 1, 4k-4m). Furthermore, when Me_4**L**^{1} was used as a catalyst, 91-95% yields and 61-80% ee were achieved for aliphatic ketones (Table 1, 4k and 4l), but only 11% yield and 56% ee were detected for the aromatic ketone (Table 1, 4m). Again, this is presumably due to that immobilizing the molecular catalysts into the MOF could generate additional steric effects around active sites, thereby increasing the level of asymmetric induction.

Chiral phosphoric acids have been shown to be highly efficient catalysts for the enantioselective reduction of C=N bonds with an organic hydride source.[19] Recently, microporous polymers and MOFs have been used to catalyze the asymmetric transfer hydrogenation of benzoxazines and ketimines, but none of them could compromise balance between clear polymeric structure and high enantioselectivities (Tables S9 and S11).[7c, 20] This promoted us to evaluate the catalytic activities of MOFs **1**-**3** in the reduction of imines. The reduction of ketimines offers a straightforward approach to produce chiral amines, which constitutes privileged building blocks for pharmaceuticals and agrochemicals.[21] To our delight, all three MOFs were found to be able to promote the ketimine reduction reactions, whereas **1** give the highest enantioselectivity. With 5 mol% loading, **1** catalyzed the reduction of (*E*)-*N*-(4-methoxyphenyl)-1-phenylethan-1-imine, giving the product 6a in 84% yield with 99% ee in toluene at 50 °C for 36 h (Table 2, 6a). The substrates with both electron-donating and withdrawing groups were compatible with this transformation, affording 86-99.9% ee. Imines with electron-withdrawing and heteroaromatic groups were also subjected to the reactions,

providing the amines in 86-93% ee (Table 2, 6b, 6d, 6e and 6f). In contrast, only 63-80% and 19-34% ee were obtained with MOFs **2** and **3** for the tested substrates, respectively, although the yields were comparable with those of **1** (Table 2, 6a-6d). Under identical conditions, the homogeneous analogue Me_4**L**^{1} produced the products in 0-39% ee values, which are substantially lower than those obtained with **1** (Table 2, 6a-6d). This further proves that bulky substituents at the 3,3'-positions of the biphenyl unit combined with the confined space of MOFs could highly enable the asymmetric activation of the substrate

Table 2 Asymmetric transfer hydrogenation reaction[a].

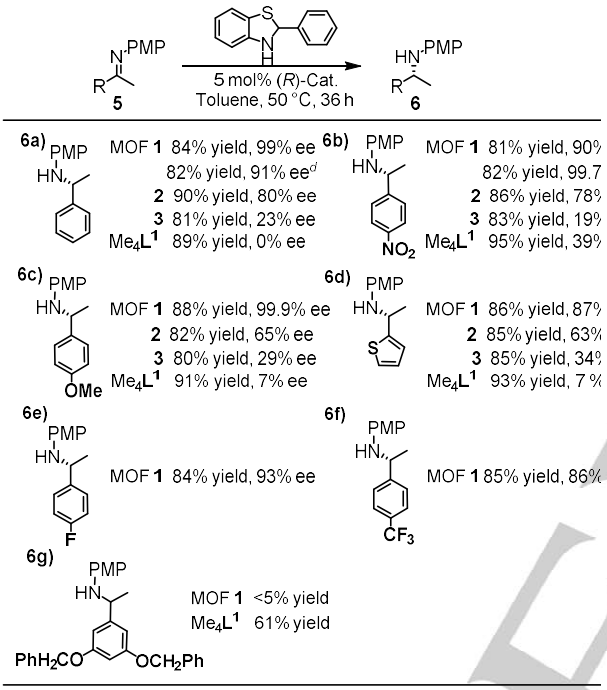

[a] Reaction conditions: **Cat**. (5 mol %), ketimine (0.15 mmol) and benzothiazoline (0.30 mmol) in toluene (1.0 mL), 50 °C, 36 h. The absolute configurations of the products were assigned as *R* by comparing their HPLC profiles with those reported in literature.[22] PMP, *p*-methoxyphenyl. [b] Isolated yield. [c] Determined by HPLC analysis. [d] The ketimines were generated *in situ.*

The major drawback of this reaction was the need for isolated ketimines, which is unstable and diffcult to synthesiz and purify. The most convenient way is to generate imines in situ for the hydrogenation reaction. As shown in Table 2, with 5 mol% loading of **1**, the reactions of different aromatic/heterocyclic ketones and aromatic amines proceeded smoothly and afforded the products in 82% yields and 91-99.7% ee in toluene at 60 ºC after 48 h. The resulting yields and ee values are comparable with those obtained from the direct reduction of ketimines catalyzed by **1**. Besides, several tests also prove that **1** is a heterogeneous and recyclable catalyst in catalyzing the imine reduction reaction (Figures 2a and S74).

In order to explore whether catalysis by **1** occurs predominantly within the channels or instead on the external surface, the more sterically demanding substituent 3,5-dibenzyloxy phenyl groups were introduced to the asymmetric condensation/amine addition and imine reduction reactions (Table 1, 4j, Table 2, 6j and Figure S7). Only trace mount of the desired products were detected by **1** even after 48 h, much lower than 45% and 61% isolated yield obtained with Me_4**L**^{1} (5 mol% loading) as the homogeneous catalyst, indicating that catalysis does not occur mainly at surface sites. This point was further supported by the fact that grounded and unground particles of **1** exhibited similar catalytic performance in asymmetric condensation/amine addition reaction.

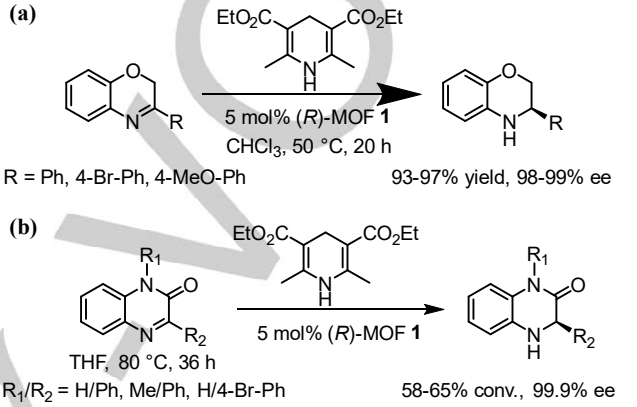

Scheme 1. Enantioselective transfer hydrogenation of (a) benzoxazines and (b) quinoxalinones.

The capability of the MOF catalyst was further demonstrated by enantioselective reduction reaction of other types of imines. For example, by using Hantzsch ester as the stoichiometric hydride source, MOF **1** was catalytically active for asymmetric transfer hydrogenation of 1,4-benzoxazines with both electron-donating and -withdrawing groups on the phenyl rings, affording the products in 93-97% yields and 98-99% ee (Scheme 1a). In addition, in the presence of using Hantzsch ester, MOF **1** could also catalyze reduction of quinoxalinones with varying substituents on the phenyl ring into the corresponding dihydroquinoxalinones in 58-65% conversions and 99.9% ee (Scheme 1b). In both cases, the ee values are comparable to those obtained with Me_4**L**^{1} (Tables S12 and S13) and other reported molecular catalysts (Tables S9 and S10),[23] but are much higher than those with MOFs **2** and **3** (80-91%, 13-51% and 11-33%, 7-24% ee). In particular, although MOFs **2** and **3** share the same less bulky substituents –phenyl at 3,3'-positions, the ee values obtained with **2** are 57-71% and 6-27% higher than those with **3**, probably due to contributions of the frameworks and the short distances between phosphoric acid sites and the frameworks.

DFT Calculations. We carried out DFT calculations to elucidate how the framework impacts on the catalytic activities. As shown in Figure S12a, one repeating unit of **1** was used in the calculations. For comparison, the homogeneous catalyst Me_4**L**^{1} was also examined. According to previously reported literatures,[24] we chose the asymmetric hydrogenation of ketimines with the imine of

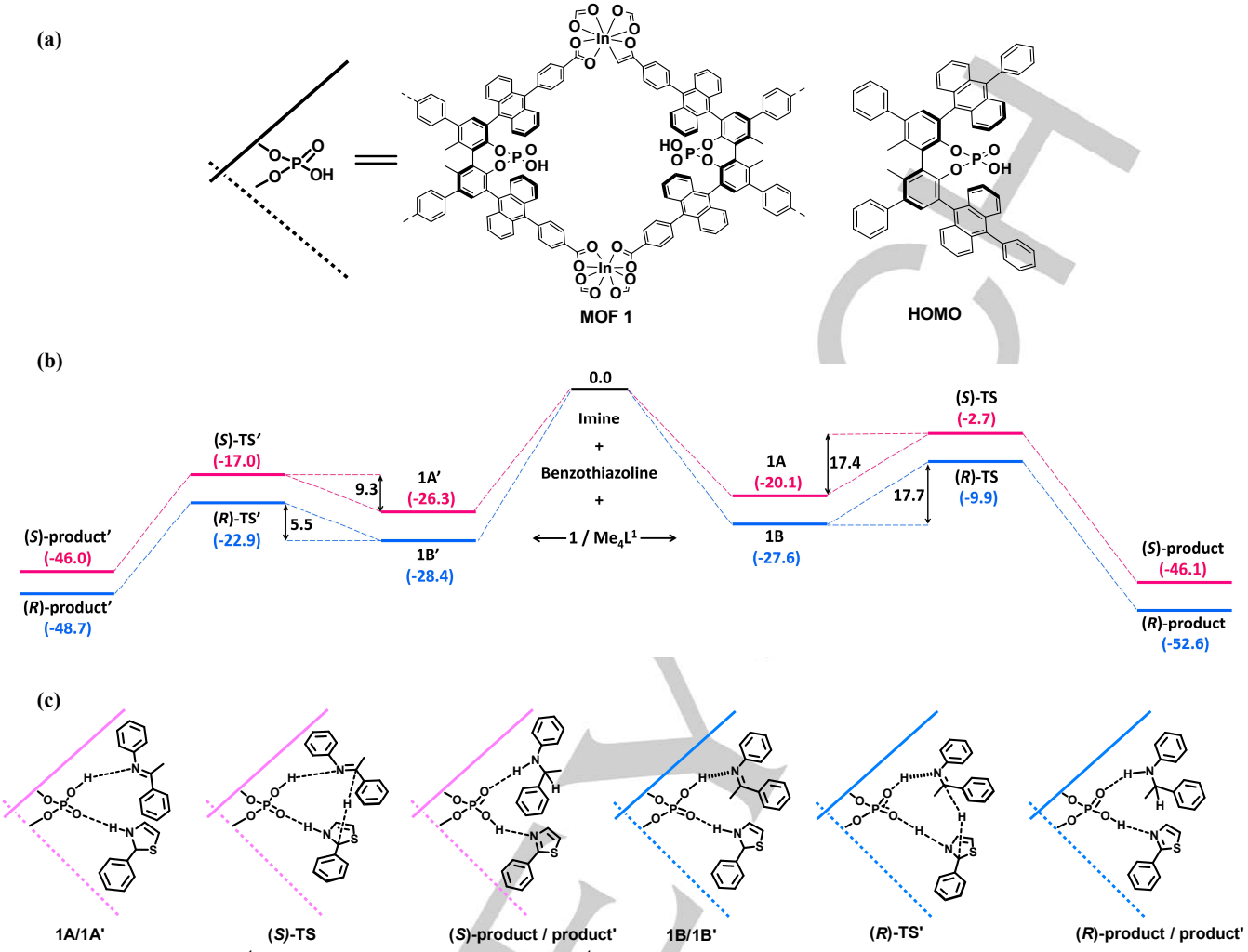

Scheme 2. (a) Simplified Me_4**L**^{1} and MOF **1**. (b) Free energies (kcal mol^{-1}) of intermediates, transition states and products in the heterogeneous (left) and homogeneous (right) system with **1** and Me_4**L**^{1}. (The pink and blue pathways are for (*S*)- and (*R*)-stereoisomers, respectively, and the reaction barrier of transition state is shown in parentheses.) (c) Schematic structures of intermediates and transition states.

acetophenone and (*R*)-benzothiazoline (simplified chemical model) as a representative example and proposed a possible catalytic cycle (Figure S12b).

In a homogeneous system with Me_4**L**^{1} (Figure S13), imine and benzothiazoline initially form intermediates with different configurations 1A and 1B and then undergo a proton transfer step to generate transition states (*S*)-TS and (*R*)-TS leading to (*S*) and (*R*)-product, respectively. As shown in Scheme 2, all the intermediates and transition states are bound on the chiral 1,1'-biphenol-2,2'-phosphoric acid through two hydrogen-bonds. Both reactions yielding (*S*) and (*R*)-product are exothermic within free energy changes of -26.0 and -25.0 kcal mol^{-1}, respectively. The reaction barrier of transition state (*S*)-TS (17.4 kcal mol^{-1}) is very close to that of (*R*)-TS (17.7 kcal mol^{-1}) (Figures S15 and S16). Therefore, both reactions have similar thermodynamics and kinetics with a low enantioselectivity. This is consistent with the experimentally observed low values of ee.

In MOF **1** (Figure S14), all the intermediates and transition states are also bound on the chiral 1,1'-biphenol-2,2'-phosphoric acid (Scheme 2). The binding energies of configurations 1A' and 1B' are -26.3 and - 28.4 kcal mol^{-1}, respectively, which are slightly stronger than configurations 1A and 1B. The two pathways to (*S*) and (*R*)-product' are also exothermic with free energy changes of -19.7 and -20.3 kcal mol^{-1}, respectively. However, the reaction barriers for transition states (*S*)-TS' (9.3 kcal mol^{-1}) and (*R*)-TS' (5.5 kcal mol^{-1}) are much lower compared to (*S*)-TS and (*R*)-TS in the homogeneous system. Thus, the reaction activity is enhanced due to confinement effect in **1**, which stabilizes the intermediates and transition states. The other striking result is that the transition state (*R*)-TS' (Figures S17 and S18) has a relatively smaller steric effect along the channel of **1**; consequently, it has a lower reaction barrier enantioselectively leading to (*R*)-product' as the major product. These calculation results are in good agreement with experimental observation and provide microscopic insight into the confinement and steric effects of MOF **1** on the activity and selectivity of asymmetric hydrogenation.

Conclusion

In summary, we have demonstrated steric protection of catalytically active sites as an efficient strategy to design MOF

with strong Brønsted acids. Incorporation of chiral phosphoric acids into MOFs leads to significant enhancement of their Brønsted acidity and endows the frameworks with high catalytic activity in the addition and reduction of imines, in which their enantioselectivities can be modulated by varying the 3,3'-substituents. DFT calculations suggest that the achieved high enantioselectivity is attributed to the confined microenvironment of catalytically active phosphoric acids in the framework. Therefore, this work lifts the constraints placed on traditional solid Brønsted acid catalysis and can lead to a new type of heterogeneous acid catalysts for the eco-friendly synthesis of fine chemicals.

Experimental Section

Full experimental procedures and DFT calculations are provided in the Supplemental Information.

Keywords: metal-organic frameworks • phosphoric acid • Brønsted acid• asymmetric catalysis • porosity

[1] M. E. Davis, *Nature* **2002**, *417*, 813-821.

[2] a) F. Su, Y. Guo, *Green Chem.* **2014**, *16*, 2934-2957; b) J. Liang, Z. Liang, R. Zou, Y. Zhao, *Adv. Mater.* **2017**, *29*,.1701139.

[3] H-U. Blaser, H-J. Federsel, Asymmetric Catalysis on Industrial Scale: Challenges, Approaches and Solutions, Second Edition, Wiley-VCH, Weinheim, **2010**.

[4] a) Y. Liu, W. Xuan, Y. Cui, *Adv. Mater.* **2010**, *22*, 4112-4135; b) M. Yoon, R. Srirambalaji, K. Kim, *Chem. Rev.* **2012**, *112*, 11961231.

[5] a) P. Wu, C. He, J. Wang, X. Peng, X. Li, Y. An, C. Duan, *J. Am. Chem. Soc.* **2012**, *134*, 14991-14999; b) Q. Han, C. He, M. Zhao, B. Qi, J. Niu, C. Duan, *J. Am. Chem. Soc.* **2013**, *135*, 10186-10189; c) K. Mo, Y. Yang, Y. Cui, *J. Am. Chem. Soc.* **2014**, *136*, 1746-1749; d) T. Sawano, P. Ji, A. R. McIsaac, Z. Lin, C. W. Abney, W. Lin, *Chem. Sci.* **2015**, *6*, 7163-7168; e) T. Shi, Z. Guo, H. Yu, J. Xie, Y. Zhong, W. Zhu, *Adv. Synth. Catal.* **2013**, *355*, 2538-2543; f) Y. Zhang, J. Guo, L. Shi, Y. Zhu, K. Hou, Y. Zheng, Z. Tang, *Sci. Adv.* **2017**;*3*: e1701162; g) J. Li, Y. Ren, C. Qi, H. Jiang, *Chem. Commun*. **2017**, *53*, 8223-8226; h) Z. Li, Y. Liu, X. Kang, Y. Cui, *Inorg. Chem.* **2018**, *57*, 9786-9789.

[6] a) C. Tan, X. Han, Z. Li, Y. Liu, Y. Cui, *J. Am. Chem. Soc.* **2018**, *140*, 16229-16236; b) T. Sawano, N. C. Thacker, Z. Lin, A. R. McIsaac, W. Lin, *J. Am. Chem. Soc.* **2015**, *137*, 12241-12248; c) M. Banerjee, S. Das, M. Yoon, H. J. Choi, M. H. Hyun, S. M. Park, G. Seo, K. Kim, *J. Am. Chem. Soc.* **2009**, *131*, 7524-7525; d) D. Dang, P. Wu, C. He, Z. Xie, C. Duan, *J. Am. Chem. Soc.* **2010**, *132*, 14321-14323; e) J. M. Falkowski, T. Sawano, T. Zhang, G. Tsun, Y. Chen, J. V. Lockard, W. Lin, *J. Am. Chem. Soc.* **2014**, *136*, 5213-5216; f) L. Ma, J. M. Falkowski, C. Abney, W. Lin, *Nat. Chem.* **2010**, *2*, 838-846; g) Q. Xia, Z. Li, C. Tan, Y. Liu, W. Gong, Y. Cui, *J. Am. Chem. Soc.* **2017**, *139*, 8259-8266;

[7] a) K. Tanaka, K. Sakuragi, H. Ozaki, Y. Takada, *Chem. Commun.* **2018**, *54*, 6328-6331; b) M. Zheng, Y. Liu, C. Wang, S. Liu, W. Lin, *Chem. Sci.* **2012**, *3.* 2623-2627; c) Z. Zhang, Y. R. Ji, L. Wojtas, W. Y. Gao, S. Ma, M. J. Zaworotko, J. C. Antilla, *Chem. Commun.* **2013**, *49*, 7693-7695; d) D. J. Lun, G. I. Waterhouse, S. G. Telfer, *J. Am. Chem. Soc.* **2011**, *133*, 5806-5809; e) M. J. Ingleson, J. P. Barrio, J. Bacsa, C. Dickinson, H. Park, M. J. Rosseinsky, *Chem. Commun.* **2008**, 1287-1289; f) L. Liu, T. Y. Zhou, S. G. Telfer, *J. Am. Chem. Soc.* **2017**, *139*, 13936-13943.

[8] a) G. K. Shimizu, R. Vaidhyanathan, J. M. Taylor, *Chem. Soc. Rev.* **2009**, *38*, 1430-1449; b) M. Taddei, F. Costantino, F. Marmottini, A. Comotti, P. Sozzani, R. Vivani, *Chem. Commun.* **2014**, *50*, 14831-14834; c) S. Kim, B. Joarder, J. A. Hurd, J. Zhang, K. W. Dawson, B. S. Gelfand, N. E. Wong, G. K. H. Shimizu, *J. Am. Chem. Soc.* **2018**, *140*, 1077-1082.

[9] a) N. Stock, S. Biswas, *Chem. Rev*. **2012**, *112*, 933-969; b) M. J. Van Vleet, T. Weng, X. Li, J. R. Schmidt, *Chem. Rev.* **2018**, *118*, 3681-3721.

[10] a) G. Ferey, C. Serre, C. Mellot-Draznieks, F. Millange, S. Surble, J. Dutour, I. Margiolaki, *Angew. Chem. Int. Ed.* **2004**, *43*, 6296-6301; *Angew. Chem.* **2004**, *116*, 6456-6461;b) G. Ferey, C. Mellot-Draznieks, C. Serre, F. Millange, J. Dutour, S. Surble, I. Margiolaki, *Science* **2005**, *309*, 2040-2041.

[11] D. Parmar, E. Sugiono, S. Raja, M. Rueping, *Chem. Rev.* **2014**, *114*, 9047-9153.

[12] a) J. P. Reid, J. M. Goodman, *Chem. Eur.J.* **2017**, *23*, 14248-14260; b) L. W. Qi, J. H. Mao, J. Zhang, B. Tan, *Nat. Chem.* **2018**, *10*, 58-64; c) W. Kashikura, K. Mori, T. Akiyama, *Org. Lett.* **2011**, *13*, 1860-1863.

[13] a) X. Chen, Y. Peng, X. Han, Y. Liu, X. Lin, Y. Cui, *Nat. Commun.* **2017**, *8*, 2171; b) X. Chen, H. Jiang, B. Hou, W. Gong, Y. Liu, Y. Cui, *J. Am. Chem. Soc.* **2017**, *139*, 13476-13482.

[14] A. L. Spek, *J. Appl. Crystallogr.* **2003**, *36*, 7-13.

[15] C. Walling, *J. Am. Chem. Soc.* **1950**, *72*, 1164-1168.

[16] a) G. M. Chinigo, M. Paige, S. Grindrod, E. Hamel, S. Dakshanamurthy, M. Chruszcz, W. Minor, M. L. Brown, *J. Med. Chem.* **2008**, *51*, 4620-4631; b) M. Badolato, F. Aiello, N. Neamati, *RSC Adv.* **2018**, *8*, 20894-20921.

[17] a) S. Ayyanar, P. K. Vijaya, M. Mariyappan, V. Ashokkumar, V. Sadhasivam, S. Balakrishnan, C. Chinnadurai, S. Murugesan, *New J. Chem.* **2017**, *41*, 7980-7986; b) D. Huang, X. Li, F. Xu, L. Li, X. Lin, *ACS Catal.* **2013**, *3*, 2244-2247; c) M. Rueping, A. P. Antonchick, E. Sugiono, K. Grenader, *Angew. Chem. Int. Ed.* **2009**, *48*, 908-910; *Angew. Chem.* **2009**, *121*, 925-927; d) P. Du, H. Zhou, G. Shen, K. Zou, *Chin. J. Org. Chem.* **2015**, *35,*1641-1649; e) X. Cheng, S. Vellalath, R. Goddard, B. List, *J. Am. Chem. Soc.* **2008**, *130*, 15786-15787; f) D.-J. Cheng, Y. Tian, S.-K. Tian, *Adv. Syn. Catal.* **2012**, *354*, 995-999; g) B. Zhang, L. Shi, R. Guo, *Catal. Lett.* **2015**, *145*, 1718-1723.

[18] Y. Jiang, Y. Liu, S.-J. Tu, F. Shi, *Tetrahedron: Asymmetry* **2013**, *24*, 1286-1296.

[19] C. Zhu, K. Saito, M. Yamanaka, T. Akiyama, *Acc. Chem. Res.* **2015**, *48*, 388-398.

[20] a) M. Rueping, E. Sugiono, A. Steck, T. Theissmann, *Adv. Syn. Catal.* **2010**, *352*, 281-287; b) C. Bleschke, J. Schmidt, D. S. Kundu, S. Blechert, A. Thomas, *Adv. Syn. Catal.* **2011**, *353*, 3101-3106; c) D. S. Kundu, J. Schmidt, C. Bleschke, A. Thomas, S. Blechert, *Angew. Chem. Int. Ed.* **2012**, *51*, 5456; *Angew. Chem.* **2012**, *12*4, 5552-5555. d) A. V. Malkov, M. Figlus, P. Kocovsky, *J. Org. Chem.* **2008**, *73*, 3985-3995.

[21] T. C. Nugent, Chiral Amine Synthesis: Methods, Developments and Applications, Wiley-VCH: Weinheim, **2010**.

[22] a) S. Hoffmann, A. M. Seayad, B. List, *Angew. Chem. Int. Ed.* **2005**, *44*, 7424-7427; *Angew. Chem*. **2005**, *117*, 7590-7593; b) R. I. Storer, D. E. Carrera, Y. Ni, D. W. MacMillan, *J. Am. Chem. Soc* .**2006**, *128*, 84-86; c) C. Zhu, T. Akiyama, *Org. Lett.* **2009**, *11*, 4180-4183; d) K. Saito, H. Miyashita, T. Akiyama, *Org. Lett.* **2014**, *16*, 5312-5315.

[23] a) M. Rueping, A. P. Antonchick, T. Theissmann, *Angew. Chem. Int. Ed.* **2006**, *45*, 6751-6755; *Angew. Chem.* **2006**, *118*, 6903; b) Y. Zhang, R. Zhao, R. L.-Y. Bao, L. Shi, *Eur. J. Org. Chem.* **2015**, 3344-3351; c) M. Rueping, F. Tato, F. R. Schoepke, *Chem. Eur. J.* **2010**, *16*, 2688-2691; d) J. L. Nunez-Rico, A. Vidal-Ferran, *Org. Lett.* **2013**, *15*, 2066-2069.

[24] a) L. Simon, J. M. Goodman, *J. Am. Chem. Soc.* **2008**, *130*, 8741-8747; b) Y. Shibata, M. Yamanaka, *J. Org. Chem.* **2013**, *78*, 3731-3736.

WILEY-VCH

RESEARCH ARTICLE

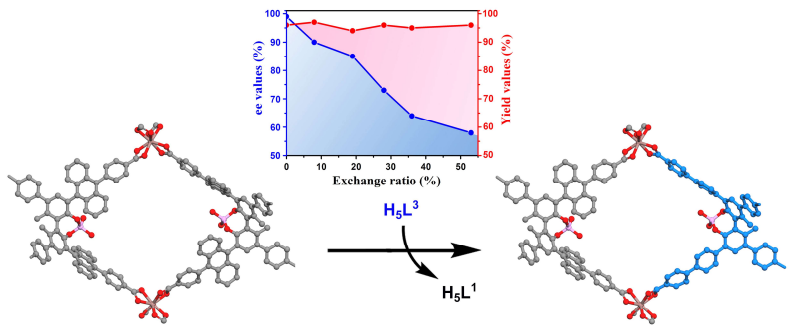

New heterogeneous Brønsted acid catalysts with high activity and selectivity are critically needed to replace precious acid-based catalysts for the sustainable production of fine and commodity chemicals, but synthetically they still face a big challenge. We report here that chiral phosphoric acids can be constructed into metal-organic frameworks (MOFs) by sterically preventing them from coordination. This leads to the synthesis of three chiral porous 3D In-MOFs with different network topology from three tetracarboxylate linkers derived from enantiopure 1,1'-biphenol-phosphoric acid. All phosphoric acid groups are uncoordinated and periodically aligned within the channels that display significantly enhanced acidity compared to non-immobilized acids. This facilitates the Brønsted acid catalysis of asymmetric condensation/amine addition and imine reduction. The enantioselectivities can be tuned (up to >99% ee) by varying substituents and have a nearly linear correlation with the concentrations of steric bulky groups in the MOFs. Density-functional theory calculations suggest that the framework provides a chiral confined microenvironment that dictates both selectivity and reactivity of the chiral MOFs.

Text for Table of Contents

Xu Chen,[a]+ Hong Jiang,[a]+ Xu Li,[b] Bang Hou,[a] Wei Gong,[a] Xiaowei Wu,[a] Xing Han,[a] Fanfan Zheng,[a] Yan Liu,[a] Jianwen Jiang,[b]* and Yong Cui[a]**

Page No. – Page No.

Chiral Phosphoric Acids in Metal-Organic Frameworks with Enhanced Acidity and Tunable Catalytic Selectivity